Analysis of Pressure Profile and Flow Progression in the Vacuum Infusion Process

Dhiren Modi, Michael Johnson, Andrew Long, Christopher Rudd

Accepted Manuscript

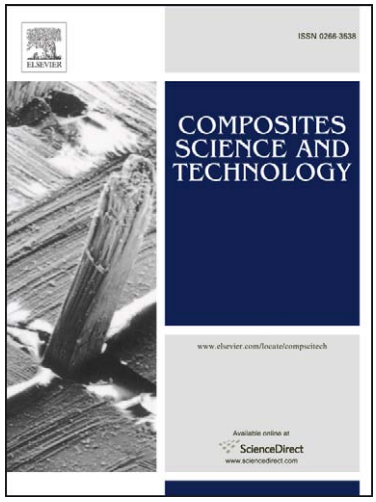

Analysis of Pressure Profile and Flow Progression in the Vacuum Infusion Process

Dhiren Modi, Michael Johnson, Andrew Long, Christopher Rudd

PII: S0266-3538(08)00231-5
DOI: 10.1016/j.compscitech.2008.05.026
Reference: CSTE 4100

To appear in: *Composites Science and Technology*

Received Date: 28 February 2008
Revised Date: 29 May 2008
Accepted Date: 30 May 2008

Please cite this article as: Modi, D., Johnson, M., Long, A., Rudd, C., Analysis of Pressure Profile and Flow Progression in the Vacuum Infusion Process, *Composites Science and Technology* (2008), doi: 10.1016/j.compscitech.2008.05.026

Analysis of Pressure Profile and Flow Progression in the Vacuum Infusion Process

Dhiren Modi, Michael Johnson, Andrew Long[1], Christopher Rudd

School of Mechanical, Materials and Manufacturing Engineering, University of Nottingham, Nottingham, NG7 2RD, UK

Abstract

New experimental set-ups are presented for measuring the pressure profile and fill-times in the Vacuum Infusion (VI) process. In these set-ups, the injection can either be from one of the mould faces (resulting in a rectilinear flow) or from a central port (resulting in a radial flow). From these measurements, the validity of previously reported analytical formulations is investigated. At the start of injection, the experimental results show a marked difference from analytical predictions. However, with flow progression, they change to match with analytical predictions. This phenomenon has not been observed previously and its analysis enhances the current understanding of the process physics, mainly the impact of compliance on the reinforcement thickness and flow progression.

Key words: Polymer-matrix composites (A), Textile composites (A), Transport properties (B), Vacuum Infusion

[1] Corresponding Author. E-mail Address: Andrew.Long@nottingham.ac.uk

1 Introduction

Vacuum Infusion is a low cost process, particularly suitable for low volume production of large parts. Compared to hand lay-up, it offers many advantages such as an emissions-free work environment, lower void content, higher fibre volume fraction etc. These, along with increasing health awareness and changing environmental regulations, are driving its popularity. The process uses a resin pressure gradient, created by evacuating the mould, to impregnate the porous preform. Due to a low working pressure range in the VI process, the mould top half is made flexible. However, during the infusion stage, the liquid pressure of the flowing resin balances off some of the compacting atmospheric pressure, thus leading to a dynamic mould cavity. The complexity of the process is increased as the preform flow properties such as the fibre volume fraction and permeability, which govern the pressure and velocity of the flowing resin, are thickness dependent. Hence, an improved understanding of the infusion stage, specifically the distribution of resin pressure and flow progression, is desirable to develop accurate mathematical and numerical models.

Many authors [1–6] have reported analytical formulations for the rectilinear (or 1D) flow VI process. Correia [6] unified these formulations to derive the formulation in Equation 1, under constant flow-rate assumption.

$$\frac{d^2P}{d\alpha^2} + \left[\frac{1}{K}\frac{dK}{dP} + \left(\frac{1-h^*\alpha}{h}\right)\frac{\partial h}{\partial P}\right]\left(\frac{dP}{d\alpha}\right)^2 = 0 \tag{1}$$

Here, P is fluid pressure, K is reinforcement permeability, h is mould thickness, L is instantaneous flow front position, α $(= \frac{x}{L})$ is non-dimensional distance and $h^* = \frac{h}{h_{\alpha=1}}$.

Modi [7] considered the variation in the flow-rate to present an improved formulation (Equation 2).

$$\frac{d^2P}{d\alpha^2} + \left[\frac{1}{K}\frac{dK}{dP} + \left(\frac{\phi+\alpha^2}{h\phi}\right)\frac{dh}{dP}\right]\left(\frac{dP}{d\alpha}\right)^2 = 0 \tag{2}$$

Here, ϕ (=1-V_f) is reinforcement porosity. The author also developed a new analytical formulation for the radial flow VI process (Equation 3).

$$\frac{d^2P}{d\alpha^2} + \left[\frac{1}{K}\frac{dK}{dP} + \left(\frac{\phi+\alpha^2}{h\phi}\right)\frac{dh}{dP}\right]\left(\frac{dP}{d\alpha}\right)^2 + \left[\frac{(R-r_{inj})}{r_{inj}+\alpha\ (R-r_{inj})}\right]\frac{dP}{d\alpha} = 0 \tag{3}$$

Here, R is the instantaneous flow front position, r_{inj} is the injection gate radius, and α ($=\frac{r-r_{inj}}{R-r_{inj}}$) is non-dimensional distance. The relationships defining the dependence of permeability (Equation 6) and thickness (Equation 7) on fluid pressure were derived using the Kozeny-Carman equation (Equation 4) and the empirical model suggested by Robitaille and Gauvin [8] (Equation 5).

$$K = k\,\frac{\phi^3}{(1-\phi)^2} \tag{4}$$

$$V_f = V_{f0}\,P_{comp}^{B}\,,\ \text{where}\ \ P_{comp} = P_{atm} - P\ \ \text{and}\ \ V_f = \frac{n\,S_d}{\rho\,h} \tag{5}$$

$$\frac{dK}{dP} = k\,B\frac{\left(-3\,P_{Comp}^{-(B+1)}\,V_{f0} + P_{Comp}^{B-1}\,V_{f0}^3 + 2\,P_{Comp}^{-2B-1}\right)}{V_{f0}^2} \tag{6}$$

$$\frac{dh}{dP} = \frac{n\,S_d\,B}{\rho\,V_{f0}\,P_{Comp}^{B+1}} \tag{7}$$

Here, k is Kozeny constant (estimated from permeability characterisation experiments), V_f is fibre volume fraction, P_{comp} is compaction pressure, P_{atm} is atmospheric pressure, n is number of reinforcement layers, S_d is reinforcement areal density, ρ is fibre density, and V_{f0} and B are compliance behaviour empirical constants (estimated from compliance characterisation experiments).

For VI, Modi [7] suggested that saturated expansion experiments should be used to estimate the values of V_{f0} and B.

As the pressure formulations (Equations 2 and 3) were coupled equations, their solutions were found using numerical methods. In addition, Modi [7] also showed that, for both 1D and 2D flow processes, the ratio of RTM and VI fill-times remains constant with flow progression, i.e. for 1D flow, the VI fill-times will vary with square of the infused length, while for 2D flow, the fill-times will vary in a similar fashion with flow progression as in RTM.

In the absence of closed form solutions, the validity of these numerical solutions can only be verified using experimental results. The majority of VI-related experimental work reported in the literature is focused on either measuring the thickness variation due to the reinforcement compliance behaviour [9,10] or measuring the lead-lag distance in the VI process with a distribution medium on top i.e. in the SCRIMP^{TM} process [11, 12]. In fact, the only experimental effort to measure pressure profiles and fill-times was reported by Correia [6]. This was to validate his analytical formulation for a 1D flow VI process. From the experimental results, the author noted that the injection pressure does not rise to its full value immediately after the start of injection, but evolves with flow progression. He attributed this evolution of the injection pressure to changes in the reinforcement permeability and the resistance of the injection pipe. He argued that one should only use the pressure results from inside the mould once the full injection pressure has been realised. Consequently, fluid pressure data acquired during saturated flow were used to validate the analytical formulation. The numerical results of the analytical formulation compared well with experimental results, and for the first time, demonstrated the pressure profile in a 1D flow VI process to be non-linear as suggested by

various formulations. Correia [6] also reported experimental validation efforts for his formulation of fill-times for the 1D flow VI process. In his experiments, the author used woven material with relatively low permeability. The resulting high variability in the experimental results of normalised fill-times vs. driving pressure prevented rigorous validation of the analytical solution.

In his experiments, Correia [6] measured fluid pressure at four locations only, including at the injection gate and the vent, to generate the expected non-linear pressure profile. By using more pressure transducers, one can increase the accuracy and also, determine the evolution of the pressure profile with flow progression. However, one can only accommodate a limited number of transducers in any given mould, as a minimum spacing need to be maintained to facilitate mounting and removal. This paper presents new experimental set-ups for continually measuring the pressure profile and fill-times in 1D and 2D, unsaturated flow VI processes. The validity of analytical formulations is also investigated through comparison with experimental results.

2 Experimental Set-up

2.1 Rectilinear (1D) Flow Set-up

In the new set-up for a 1D flow VI process, the top half was made from an aluminium frame (Figure 1). Using a sealant tape, a flexible polymeric bag was attached to the top side of this frame, while a 'P' shaped draught excluder was attached its mould side. The use of a draught excluder allows one to make a flexible mould sealing arrangement for easy, fast and repeatable experiments. After placing the reinforcement on the mould bottom half, made from a 25

mm thick clear perspex sheet, it was covered with the mould top half. The transducers (Part: 348-8093, RS Components Ltd., UK [2]), with a housing diameter of 25 mm, need to be spaced apart by at least 50 mm to allow easy installation and removal. A total of eight transducers, including one at the injection and the vent lines, were used in the mould such that at least five of them were in the first 100 mm of the infused length. In addition, the pressure port of transducers, 6 mm in diameter and 30 mm long, needs to be completely filled to sense the fluid pressure. Hence, to ensure faster sensing of fluid arrival at any pressure transducer, a liner was placed inside each transducer (Figure 1) pressure port. To create exact injection conditions for a 1D flow, a groove was cut in the mould. A 'C' shaped channel (Figure 1), with a centre hole for fluid injection, was placed inside this groove to serve as an injection line. The channel height was set such that the open section of the channel remained in line with the reinforcement.

Then, starting the vacuum pump evacuated the mould, driving infusing fluid through the injection line. The fluid injected from the centre hole first filled the channel before starting to infuse the reinforcement. This ensured that the fluid was injected through the entire thickness of the reinforcement.

2.2 Radial (2D) Flow Set-up

In the radial flow VI process, the design of the mould top and bottom halves and the pressure transducer liner were identical to the 1D case (Figure 2). Also, the same transducers were used. By aligning transducers along different radial axes, a total of eight transducers, including one at the injection gate

[2] http://rswww.com

and one at the vent, were used such that five transducers were in a radius of 100 mm from the injection gate. To prevent the vacuum bag from blocking the injection gate by sagging into it, a small, rigid piece of plastic (2 mm thick) was placed between the reinforcement and the plastic bag, directly above the injection gate. A centre hole, of 5 mm radius, was cut into the reinforcement to create uniform plug-flow injection conditions.

Before the start of experiments, all transducers were calibrated for the full pressure range. Then, in all experiments, the atmospheric pressure was assumed to be 0 kPa (i.e. 100 kPa-absolute), while the pressure at the injection and the vacuum port was maintained at 5 kPa (i.e. 95 kPa absolute) and 65 kPa (i.e. 35 kPa-absolute) below atmospheric pressure, respectively. Thus, the maximum driving pressure was 60 kPa, while the maximum and minimum compaction pressures on the reinforcement were 65 kPa and 5 kPa, respectively. A computer connected through a data acquisition box logged the transducer readings at a sampling frequency of 10 Hz. All the experiments were recorded with a digital camera at a rate of 30 frames per second, with images analysed manually to calculate fill-times.

In total, four experiments each, for both 1D and 2D flow cases, were performed using a continuous filament random mat (Unifilo U750/375, 0.375 $Kg\,m^{-2}$, 4 layers). The infusing fluid (hydraulic oil, HDX 30, Trent Oil Ltd., UK) was drawn from a bucket, using a 0.5 metre long plastic injection pipe. All infusion experiments were performed in a climate controlled room with a set temperature of 18 ^{0}C. Nonetheless, in all experiments, the temperature of the infusing medium (hydraulic oil) was also measured before the start of the injection and did not show any major variations. A Brookfield rheometer (model DV-II) was used to measure the viscosity at this temperature, providing a value of 0.3 Pa

S, which was used for comparing the experimental and predicted fill-times results.

3 Results and Discussion

3.1 Pressure Profile Results

Figure 3 shows typical results of pressure measurements in 1D and 2D flow VI processes. It is clear that in the 1D flow process, realisation of the full injection pressure is not immediate at the start of injection but needs some time. Correia [6] reported similar results and showed that the rise in the injection pressure depends on the reinforcement permeability and the flow resistance in the injection pipe. The immediate rise in the injection pressure in 2D flow experiments, using an identical set-up and reinforcement, show that the type of flow is also a contributing factor.

Figures 4 and 5 show an average pressure profile and its evolution with flow progression in 1D and 2D flow VI processes, along with the scatter in results from four identical experiments. The RTM and VI analytical pressure profiles were calculated using Equations 8-9 and Equations 2-3, respectively. The injection pressure was assumed to be equal to the instantaneous experimental injection pressure, while the values of V_{f0} and B were taken to be 0.060 and 0.117 from saturated expansion experiments [6].

$$P = P_{inj}\left(1 - \frac{x}{L}\right) \tag{8}$$

$$P = P_{inj}\left(\frac{ln\left(\frac{r}{R}\right)}{ln\left(\frac{r_{inj}}{R}\right)}\right) \tag{9}$$

In both flow processes, the initial pressure profile in the filled region is below the RTM analytical pressure profile (Figures 4-a & 5-a). Furthermore, with flow progression, the pressure profile in the 1D flow process levels with the RTM pressure profile (Figures 4-b,c) before rising above it to give a non-linear pressure profile (Figure 4-d). In radial flow, although the pressure profile has not risen to match with analytical predictions, a trend similar to 1D flow experiments is observed. This dynamic behaviour in pressure profiles is contrary to one's expectation. Note that the discrepancy between the RTM and VI analytical profiles is due to flexible top half of the mould in VI. This is well-known and well-documented in literature [1–7].

As the analytical formulations were derived using fundamental laws (i.e. conservation of mass law and Darcy's law) without any limiting assumptions [7] and the experimental results from both flow experiments show a rising behaviour that leads to converging pressure profiles towards the analytical solutions, one can justly assume the validity of both of them. Furthermore, the evolution of injection pressure as a possible explanation for this behaviour in invalidated by radial flow experiments, where full injection pressure is achieved immediately after the start of injection. Hence, it can be concluded that the observed pressure profile variation is a consequence of the process physics. As the analytical pressure formulations did not show any transient terms, the variation in the pressure profile can only be explained through the reinforcement compliance behaviour. Considering the actual events in the compliance characterisation experiments [6], first a pre-wetted reinforcement was compacted to the required degree between two solid tool surfaces. During this phase, extra fluid in the intra-tow and inter-tow spaces was forced out. Then, during the expansion or unloading phase, the tools were moved apart mechanically to

remove the compaction pressure. However, no fluid was available at this stage to fill the empty spaces created due to the reinforcement expansion. Hence, it can be concluded that during the expansion phase, a significant proportion of the load was supported by the reinforcement (Figure 6-a).

In the actual VI process, the flexible bag is supported at the fibre/tow contact points, while it sags (i.e. is pulled or deformed) into in the inter-tow spaces. The reinforcement compaction is also due to this sagging and the related tension in the plastic bag (Figure 6-b). After fibre wetting and compaction due to the arrival of fluid, the rising fluid pressure acts against the atmospheric compaction pressure. In addition, it also reduces the bag sagging, leading to a further reduction in reinforcement compaction. It is clear that at least some, if not all, of the compaction pressure is supported by the infiltrating fluid. In addition, the stresses in the plastic bag may be important. This difference in events may lead to a different compliance behaviour, possibly resulting in a different empirical model that will enable one to explain the rising pressure profile in both the flow cases. However, it is clear that to verify this hypothesis, one will need to conduct a new set of compliance characterisation experiments.

3.2 Fill-times Results

Figure 7 shows fill-times ratio with flow progression for 1D and 2D flow processes along with scatter from four experiments. RTM fill-times were calculated using Equations 10 and 11. For this, the porosity was calculated using Equation 5. The values of V_{f0}, B, P_{Comp} and K were taken to be 0.035, 0.150

(from dry compaction experiments), 65 kPa, and 10^{-9} m^2 [13], respectively.

$$t_{RTM} = \frac{\mu\phi L^2}{2K\Delta P} \tag{10}$$

$$t_{RTM} = \frac{\mu\phi}{2K\Delta P}\left[R^2 \ln\left(\frac{R}{r_{inj}}\right) - \frac{1}{2}\left(R^2 - r_{inj}^2\right)\right] \tag{11}$$

It is clear that contrary to analytical predictions of constant fill-times ratio, it changes in both processes. Correia [6] reported similar results for 1D flow and attributed it to the variation in the injection pressure. However, 2D flow experiments, where full injection pressure is realised at the start of injection, also exhibit a similar variation. Hence, it can be concluded that the variation in the pressure profile rather than variation in the injection pressure is responsible for this behaviour. As a result, the VI fill-times for 1D flow will not vary with square of the infused length, while for 2D flow, the fill-times will not vary in a similar fashion with flow progression as in RTM.

In addition, as the pressure profile in 1D flow VI converges towards the analytical prediction, the fill-times ratio also converges to a single value. For 2D flow VI, although the pressure profile in VI is below RTM, it is reasonable to expect that once it converges to analytical prediction, it will lead to a convergence in the fill-times ratio.

Furthermore, it is clear that the experimental fill-times ratio depends on the assumed value of reinforcement permeability for RTM fill-times calculations in Equations 10 and 11. This is the reason behind the difference in absolute values of analytical (Modi [7]) and experimental fill-times ratios (Figure 7).

4 Conclusions

The lack of published experimental validation of pressure and fill-times formulations, in particular for unsaturated flow VI processes, is highlighted. Two new mould set-ups were developed for measuring pressure profiles, their evolution with flow progression and fill-times in unsaturated flow 1D and 2D VI processes. In these new set-ups, eight pressure transducers were arranged such that at least five of them could be incorporated in the first 100 mm of the infused length. This facilitated accurate reconstruction of the expected non-linear pressure profiles as well as measurement of the pressure profile evolution with flow progression.

The results showed that, in 1D flow VI process, the full injection pressure is not realised immediately. Also, the pressure profile is initially lower than the RTM pressure profile. With flow progression, it rises to level with and ultimately exceed the RTM pressure profile. A similar trend is also observed in 2D flow VI process, even though full injection pressure is realised at the start of the injection. This is in contrast to analytical formulations, which suggest that the fluid pressure profile should remain constant or move in a similar direction as the corresponding RTM profile. Hence, it is concluded that this variation in the pressure profile is an integral part of the process physics. It was hypothesised that the time-dependent pressure profile evolution is due to the difference in events in the reinforcement compliance characterisation and actual VI experiments and hence, the current empirical model for the reinforcement compliance may not be appropriate for VI. However, this hypothesis cannot be verified at present due to the lack of accurate saturated expansion data and this should be investigated in future.

In addition, results showed that, for 1D flow VI process, fill-times is not proportional to the square of the infused length. A similar observation in the radial flow VI process showed that fill-times in VI is higher than in the RTM process. This variation, in direct relation to the pressure profile evolution, invalidated the previous understanding that this deviation in fill-times, from analytical predictions, was entirely due to the evolution of the injection pressure.

Acknowledgements

The authors would like to thank the Engineering and Physical Sciences Research Council (EPSRC), which funded this research via the Nottingham Innovative Manufacturing Research Centre (NIMRC).

References

[1] A. Hammami, B. Gebart, A model for the vacuum infusion molding process, Plastics, Rubber and Composites 27 (4) (1998) 185–189.

[2] A. Hammami, B. Gebart, Analysis of the vacuum infusion molding process, Polymer Composites 21 (1) (2000) 28–40.

[3] K. Han, S. Jiang, C. Zhang, B. Wang, Flow modeling and simulation of scrimp for composites manufacturing, Composites Part A 31 (1) (2000) 79–86.

[4] M. Kang, W. Lee, H. Hahn, Analysis of vacuum bag resin transfer molding process, Composites Part A 32 (11) (2001) 1553–1560.

[5] H. Andersson, T. Lundstorm, B. Gebart, Numerical model for vacuum infusion manufacturing of polymer composites, International Journal of Numerical Methods for Heat & Fluid Flow 13 (3) (2003) 383–394.

[6] N. Correia, Analysis of the vacuum infusion moulding process, Ph.d. thesis, University of Nottingham, Nottingham, UK (2004).

[7] D. Modi, Modelling and active control of the vacuum infusion process for composites manufacture, Ph.d. thesis, University of Nottingham, Nottingham, UK (2008).

[8] F. Robitaille, R. Gauvin, Compaction of textile reinforcements for composites manufacturing. i: Review of experimental results, Polymer Composites 19 (2) (1998) 198–216.

[9] C. Williams, S. Grove, J. Summerscales, The compression response of fibre-reinforced plastic plates during manufacture by the resin infusion under flexible tooling method, Composites Part A 29 (1-2) (1998) 111–114.

[10] H. Andersson, T. Lundstorm, B. Gebart, P. Synnergren, Application of digital speckle photography to measure thickness variations in the vacuum infusion process, Polymer Composites 24 (3) (2003) 448–455.

[11] R. Mathur, D. Heider, C. Hoffman, J. Gillespie, B. Fink, Flow front measaurements and model validation in the vacuum assisted resin transfer molding process, Polymer Composites 22 (4) (2001) 477–490.

[12] A. Ragondet, Experimental characterisation of the vacuum infusion process, Ph.d. thesis, University of Nottingham, Nottingham, UK (2005).

[13] C. Rudd, A. Long, K. Kendall, C. Mangin, Liquid Moulding Technologies, Woodhead, Cambridge, UK, 1997.

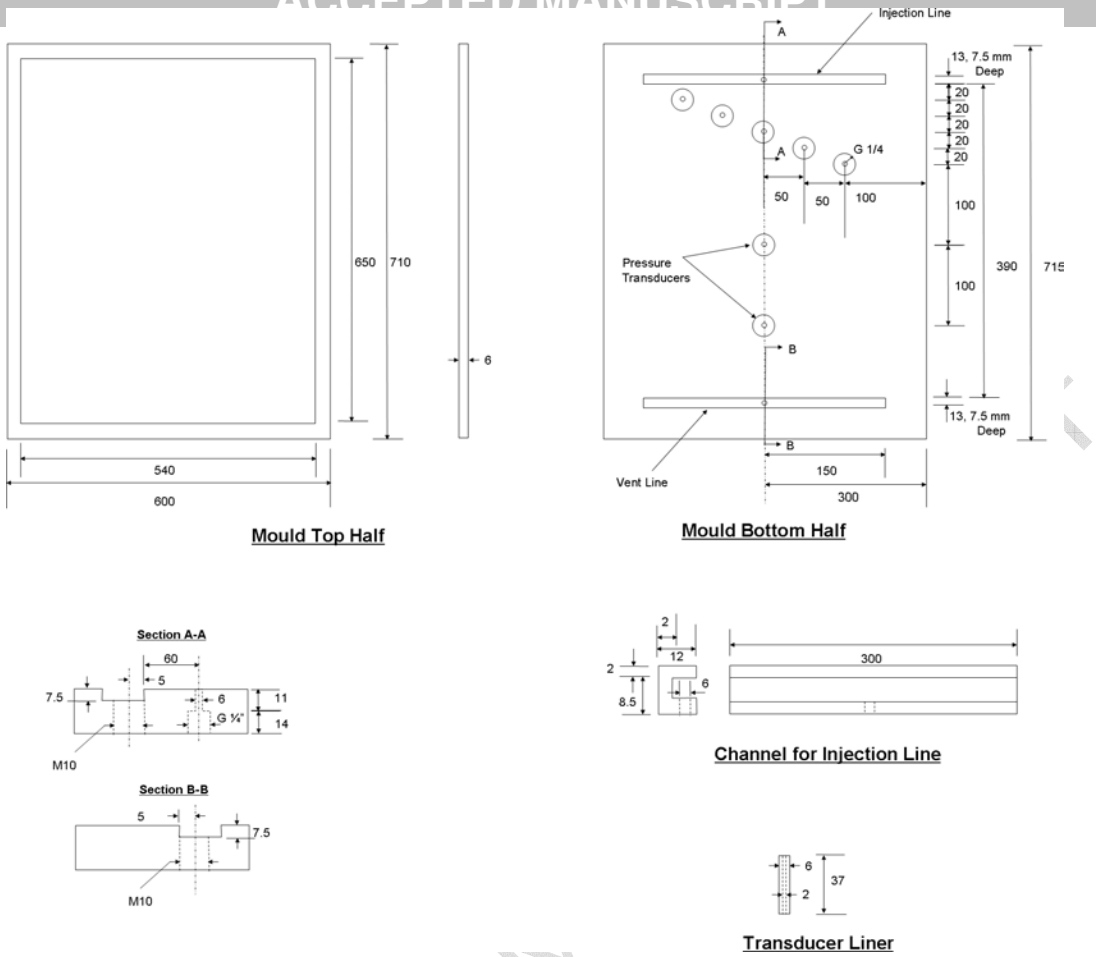

Figure 1. Experimental set-up for the rectilinear (1D) flow VI process. More pressure transducers are accommodated in this set-up by placing them across the width of the mould.

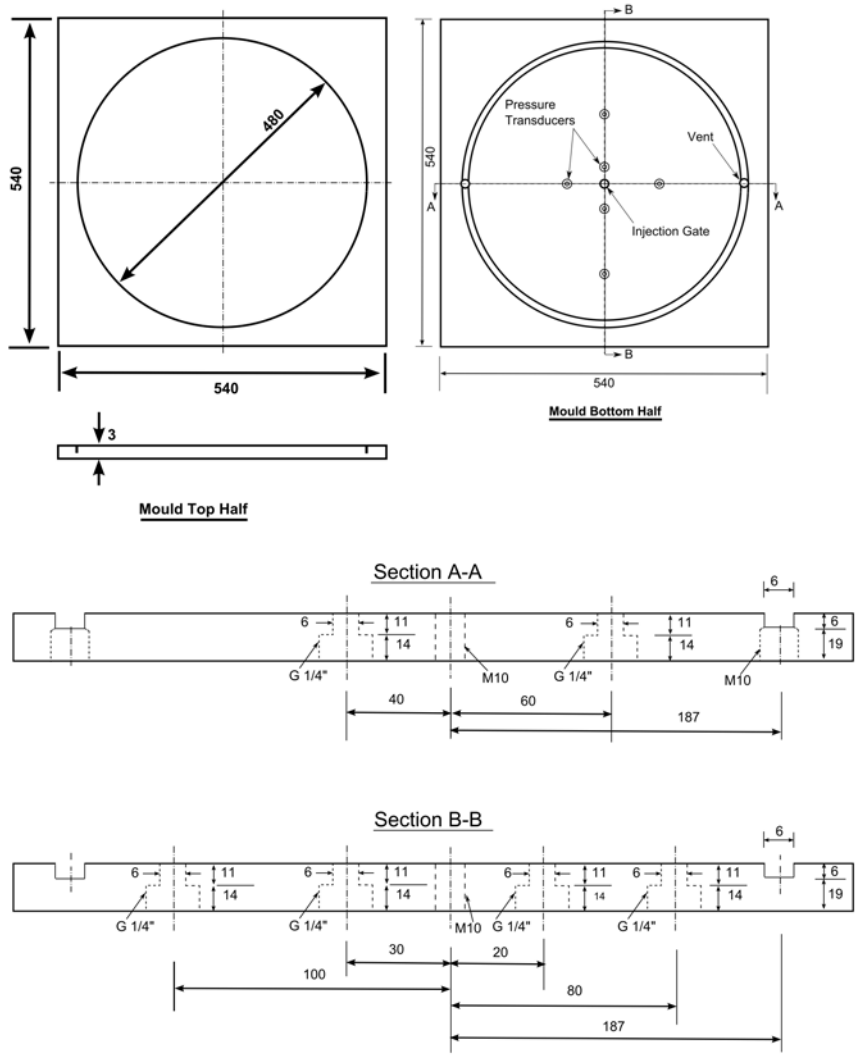

Figure 2. Experimental set-up for the radial flow VI process.

(a) Rectilinear Flow

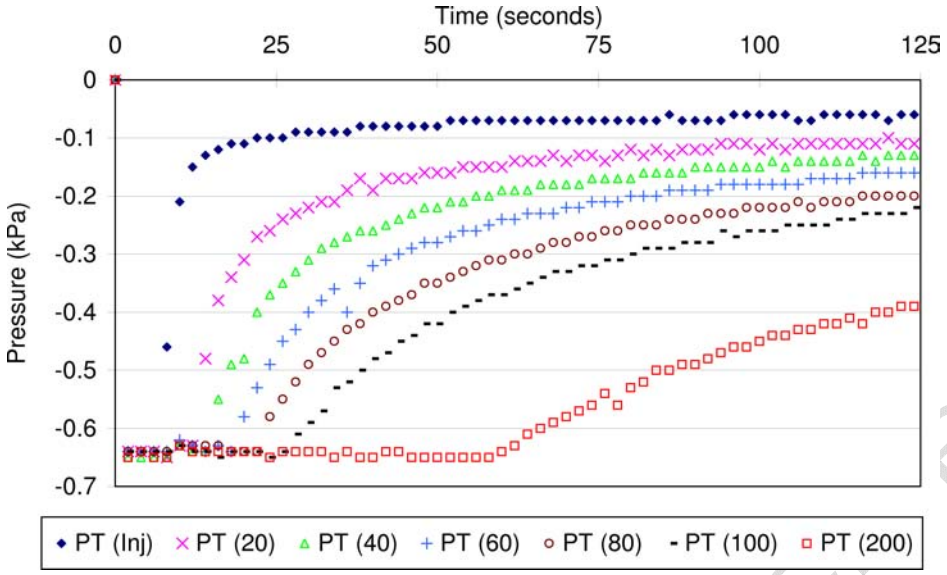

(b) Radial Flow

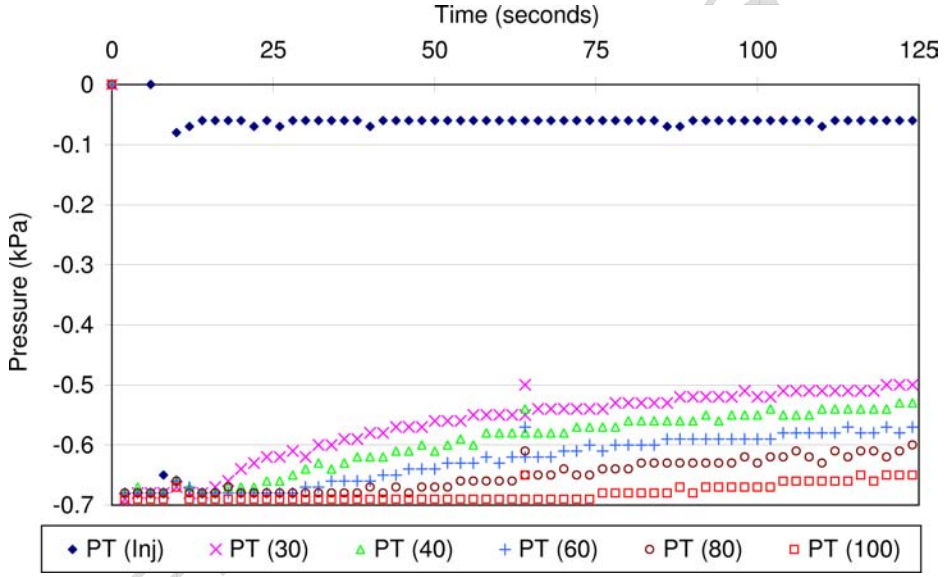

Figure 3. Pressure measurements in the rectilinear and the radial flow VI processes. The location of any pressure transducer (PT) from the injection gate is signified by the number in bracket, e.g. PT(20) = pressure transducer located at 20 mm from the injection gate.

(a) Infused Length = 60 mm

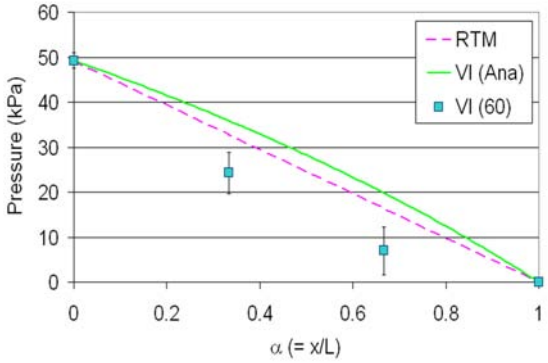

(b) Infused Length = 100 mm

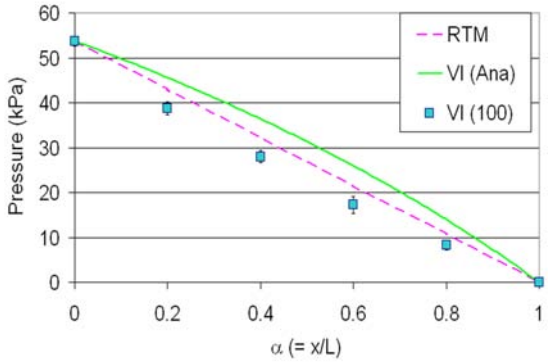

(c) Infused Length = 200 mm

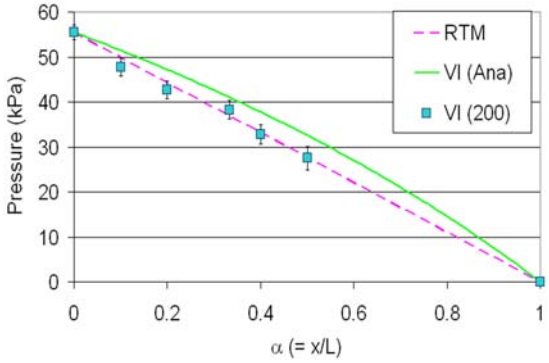

(d) Infused Length = 300 mm

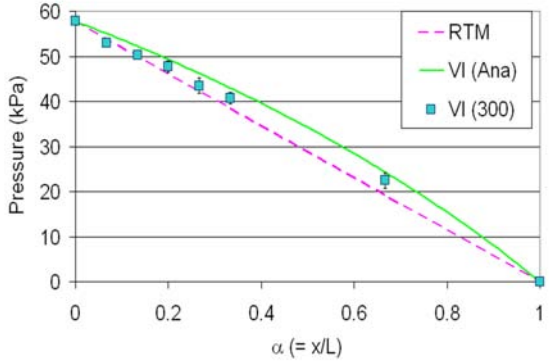

Figure 4. Pressure profile evolution with flow progression in the rectilinear flow VI experiments.

(a) Infused Radius = 80 mm

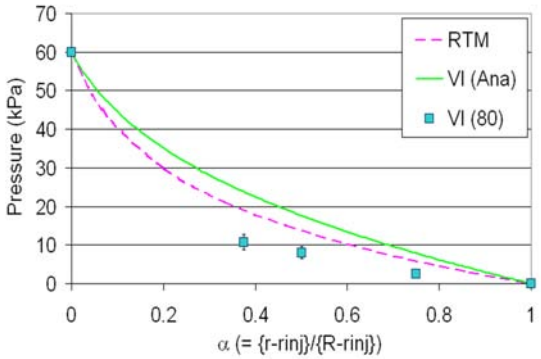

(b) Infused Radius = 100 mm

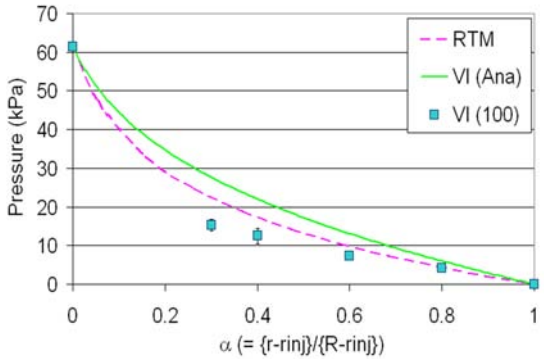

(c) Infused Radius = 160 mm

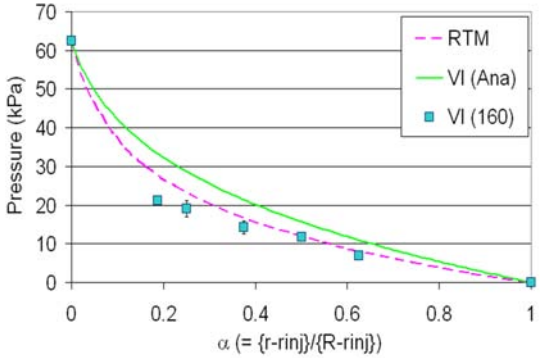

Figure 5. Pressure profile evolution with flow progression in the radial flow VI experiments.

(a) Events in the Reinforcement Compliance Experiment

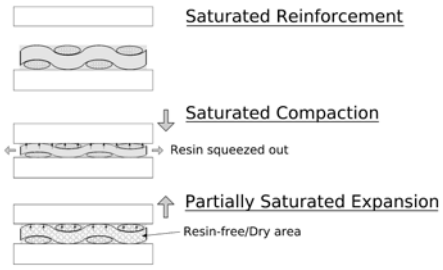

(b) Events in the Actual VI Process

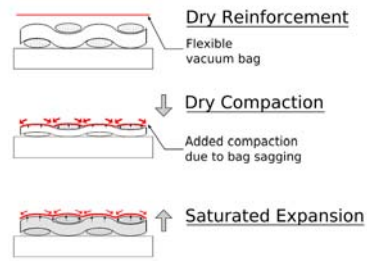

Figure 6. Comparison of events in the reinforcement compliance experiment and the actual VI process.

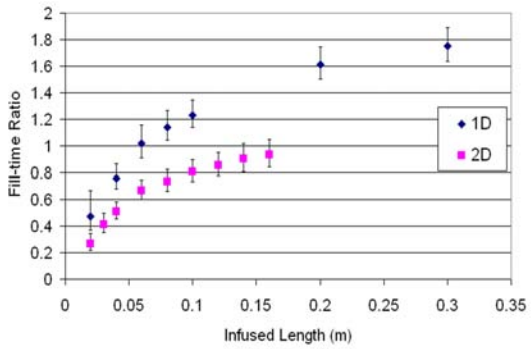

Figure 7. RTM vs. VI fill-times ratios calculated as a function of flow progression in the rectilinear and the radial flow processes.